Author/s:
Gao, C;Seow, JY;Zhang, B;Hall, CR;Tilley, AJ;White, JM;Smith, TA;Wong, WWH

Title:
Tetraphenylethene 9,10-Diphenylanthracene Derivatives – Synthesis and Photophysical Properties

Date:
2019-06-01

Citation:
Gao, C., Seow, J. Y., Zhang, B., Hall, C. R., Tilley, A. J., White, J. M., Smith, T. A. & Wong, W. W. H. (2019). Tetraphenylethene 9,10-Diphenylanthracene Derivatives – Synthesis and Photophysical Properties. Chempluschem, 84 (6), pp.746-753. https://doi.org/10.1002/cplu.201900100.

Persistent Link:
https://hdl.handle.net/11343/290244

Title: Tetraphenylethene 9,10-Diphenylanthracene Derivatives – Synthesis and Photophysical Properties

Authors: Can Gao; Jia Yi Seow; Bolong Zhang; Christopher Hall; Andrew Tilley; Jonathan White; Trevor Smith; Wallace Wing Ho Wong, Dr.

To be cited as: ChemPlusChem 10.1002/cplu.201900100

Link to VoR: https://doi.org/10.1002/cplu.201900100

Tetraphenylethene 9,10-Diphenylanthracene Derivatives – Synthesis and Photophysical Properties

Can Gao,[a] Jia Yi Seow,[a] Bolong Zhang,[a] Christopher R. Hall,[a] Andrew J. Tilley,[a] Jonathan M. White,[b] Trevor A. Smith,*[a] and Wallace W. H. Wong*[a]

Abstract: A series of tetraphenylethene 9,10-diphenylanthracene (TPE-DPA) derivatives have been synthesized, and their photophysical properties have been studied. Photoluminescence measurements in PMMA, neat films and nanoparticle dispersions reveal that different aggregation states are formed, which leads to different photophysical behaviour. The triplet excited state properties were studied using Pt(II) octaethylporphyrin (PtOEP) as triplet sensitizer. Upconverted emission from the DPA moiety is observed in nanoparticle dispersions of each derivative. A higher upconverted emission intensity is observed in aerated (compared to deaerated) solutions of the derivatives following irradiation, which we attribute to oxidation of the TPE moiety. These results provide valuable insight for the design of AIE luminogens for triplet-triplet annihilation upconversion (TTA-UC).

Introduction

Tetraphenylethene (TPE) and 9,10-diphenylanthracene (DPA) are aromatic chromophores with well-known photophysical properties that have found application as building blocks in dyes for biological imaging, chemical sensing and light harvesting.[1, 2 3-7] Anthracene is an exceptionally well-studied organic fluorophoree due to its high fluorescence quantum yield, strong light absorption, and its energetically useful triplet energy. When substituted at the 9- and 10-positions (e.g. DPA), anthracene derivatives have improved photostability and solubility, which has opened up new applications for this dye in singlet exciton fission, and triplet-triplet annihilation upconversion (TTA-UC) applications.[8-10] For studies of intramolecular TTA-UC, DPA is considered a prototypical emitter and has been incorporated within linear and star-shaped pendant polymers, oligomers and dendrimers.[4, 11-13]

TPE is a well-known aggregation induced emission (AIE) backbone that is able to exhibit AIE behaviour when coupled to a variety of chromophores. A series of luminogens composed of TPE and various aromatic hydrocarbons, such as pyrene, anthracene and naphthalene have been reported.[14-16] All the TPE-based luminogens are almost non-emissive in solution, but their solid-state films exhibit significantly enhanced photoluminescence (PL) quantum yields (Φ_{PL}). TPE derivatives thus show great potential in solid-state photoluminescent applications and other related fields.[17-22]

In this work, we designed and synthesized a series of covalently-linked dimeric and tetrameric dyes composed of a TPE core and flanking DPA units (Scheme 1). The mono-, cis- and gem-DPA were successfully synthesized and showed some unexpected properties, whereas the tetra-substituted analogue was too unstable to be practically useful. The photophysical properties of the derivatives were examined in solution, thin film, within host matrices, and in nanoparticle dispersions. With PtOEP as the triplet sensitizer, the TPE-DPA derivatives were examined as emitters for TTA-UC, both in solution and in nanoparticle dispersions. Interestingly, we find that the solution Φ_{PL} of the TPE-DPA derivatives increases after irradiation, attributed to oxidation of the TPE core to the 1,2-endoperoxide adduct. We further demonstrate that TTA-UC emission of these TPE-DPA derivatives can be switched on after irradiation in the presence of oxygen, which has implications for the use of such luminogens in TTA-UC schemes.

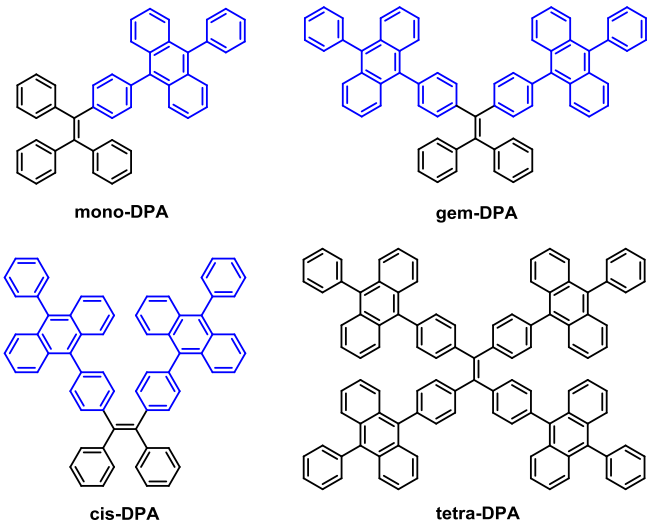

Scheme 1. Chemical structures of the TPE-DPA derivatives.

Results and Discussion

[a] C. Gao, J. Y. Seow, B. Zhang, Dr. C. R. Hall, Dr A. J. Tilley, Assoc. Prof. T. A. Smith, Dr. W. W. H. Wong
School of Chemistry, ARC Centre of Excellence in Exciton Science
The University of Melbourne
Parkville, Victoria, 3010 (Australia)
E-mail: trevoras@unimelb.edu.au; wwhwong@unimelb.edu.au
[b] Prof. J. M. White
School of Chemistry, Bio21 Institute, The University of Melbourne
Parkville, Victoria, 3010 (Australia)

Supporting information for this article is given via a link at the end of the document.

Synthesis and characterization

The TPE-DPA derivatives were synthesized by Suzuki-Miyaura coupling between boronic acid derivatives and bromo-anthracene derivatives. Full details are provided in the Experimental Section and Supporting Information. While the mono-, cis- and gem-DPA could be successfully synthesized and isolated, we found that tetra-DPA was highly unstable in air, and under UV-light. A detailed discussion of the photostability of these materials, and their susceptibility to aerial oxidation, is given in the Results and Discussion section.

Single crystal X-ray structures for the three TPE-DPA derivatives are shown in Figure 1. In cis- and gem-DPA, the anthracene cores are non-overlapping. In cis-DPA, the DPA moieties make an angle of 65.0° to each other, and are ~3.7 Å apart at their closest point. In gem-DPA, the DPA moieties make an angle of 115°, and are spaced no closer than ~8.1 Å. The intermolecular DPA-DPA and DPA-TPE distances have also been measured. The DPA-DPA distance is 7.35 Å in mono-DPA, 8.13 Å in cis-DPA, while a larger distance of 9.69 Å is observed in gem-DPA. In each derivative, DPA and TPE have a close intramolecular separation (4.89 Å in mono-DPA, 4.95 Å in cis-DPA and 4.90 Å in gem-DPA) (Table S1). The dihedral angles between ethene of the TPE and the phenyl group connected to the anthracene are 62˚, 54˚ and 56˚ for mono-, cis- and gem-DPA, respectively. Further, the dihedral angles between the phenyl group and the anthracene are 69˚, 81˚ and 82˚ for mono-, cis- and gem-DPA, respectively. Given these dihedral angles, the TPE and DPA moieties are likely to behave as separate chromophores.

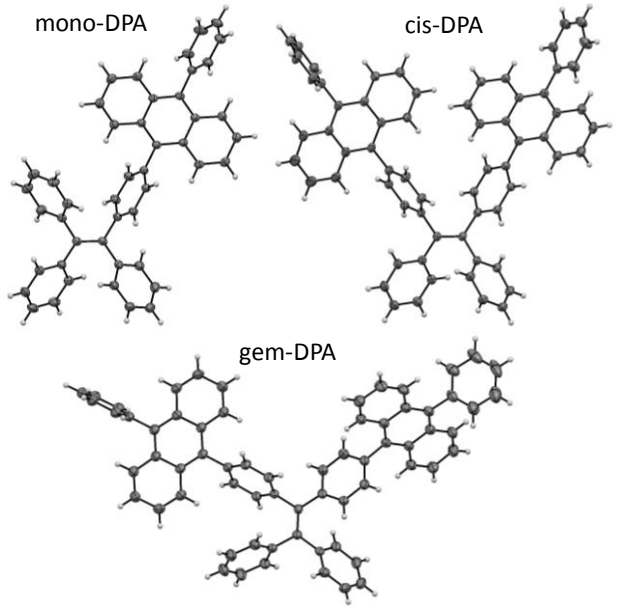

Figure 1. Thermal ellipsoid illustrations of single crystal X-ray structures of mono-DPA, cis-DPA and gem-DPA at 50%, 20% and 50% probability level respectively.

Photophysical characterization

The photophysical properties of the TPE-DPA derivatives were comprehensively studied in THF solution, PMMA thin films, and nanoparticle dispersions (Figures 2 and 3). In THF, the absorption spectra of the TPE-DPA derivatives show contributions from both the DPA and TPE moieties (Figure 2). In each case, the three vibronic bands characteristic of DPA are clearly present between 350-400 nm, while absorption by the TPE moiety contributes to the broad absorption below 350 nm. The observation of absorption features closely matching those of DPA suggests that the DPA chromophores in gem- and cis-DPA are not strongly interacting. This is consistent with the X-ray crystal structures, which show negligible intramolecular π-π interactions between the DPA chromophores in gem- and cis-DPA.

The TPE-DPA derivatives are weakly photoluminescent in solution (Figure 2 and Table 2). The emission spectrum of each derivative has lost the vibronic band structure of the DPA emission spectrum, and, in the case of cis- and gem-DPA, is red-shifted with respect to mono-DPA. The emission spectrum of mono-DPA is blue-shifted with respect to DPA, suggesting a greater contribution to the emission spectrum from TPE than for the disubstituted congeners.

The absorption properties measured in THF solution are largely retained in the PMMA films (Figure 3a). The emission spectra and photoluminescent quantum yields of each derivative are similar (see also Table 1), possibly due to restricted internal rotation within the TPE core. The similarity of the absorption and emission spectra of each TPE-DPA derivative with respect to DPA suggests that the molecules are isolated (non-aggregated) within the PMMA matrix. In the nanoparticles, the TPE-DPA derivatives show a broader and more red-shifted emission compared with the THF solutions, which is attributed to aggregation within the particles (Figure 3b).

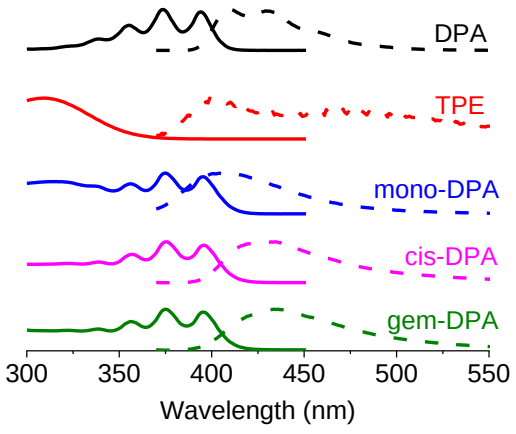

Figure 2. Normalized absorption (solid traces) and emission (dashed traces) spectra in THF solution. (λ_{ex} = 320 nm for TPE, λ_{ex} = 375 nm for DPA, mono-, cis- and gem-DPA).

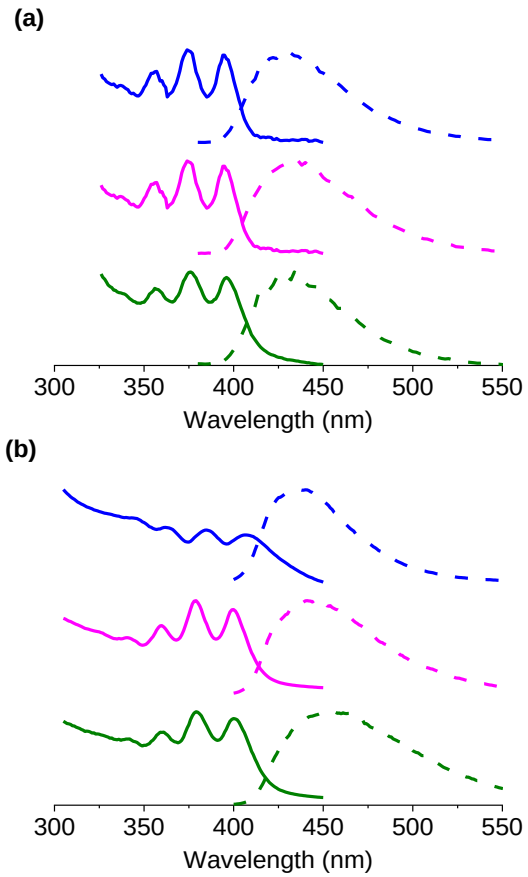

Figure 3. Normalized absorption (solid traces) and emission (dashed traces) spectra in (a) PMMA film and (b) aqueous nanoparticle dispersions of mono-, cis- and gem-DPA. (λ_{ex} = 375 nm for mono-, cis- and gem-DPA).

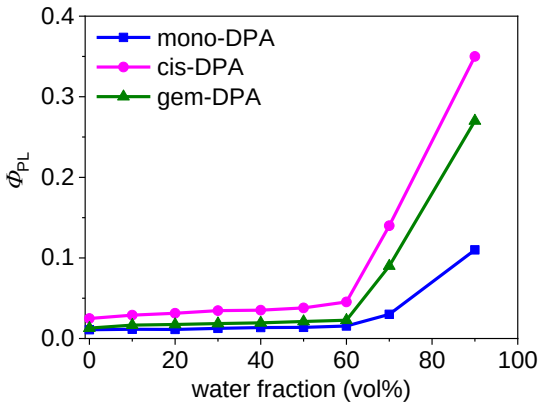

Figure 4. PL quantum yields of TPE-DPA derivatives vs. solvent composition of the water-THF mixture. ([DPA-subunit]: 40 μM. λ_{ex}: 375 nm.)

Aggregation induced emission

The functionalization of emissive chromophores with TPE can promote AIE, and thus we explored whether this property was a feature of the TPE-DPA derivatives. The AIE properties were studied by measuring the Φ_{PL} in water:THF mixtures of different ratios (Figure 4). In 0 - 60% water:THF mixtures, the Φ_{PL} values were measured by using DPA as the reference, which has a Φ_{PL} = 0.94 in dilute THF solution.[23] In 70% and 90% water-THF mixtures, the Φ_{PL} values were measured in a calibrated integrating sphere. The Φ_{PL} value remained almost unchanged when up to 60% water was added to the THF solution but started to swiftly increase afterwards. When the water fraction was increased to 90%, Φ_{PL} increased to 0.11 for mono-DPA, 0.35 for cis-DPA, and 0.27 for gem-DPA, which are 11 times, 14 times and 20 times higher than the corresponding THF solutions. The trajectory of the Φ_{PL} changes suggest that aggregation begins at a water fraction of 70%, and that the population of aggregates (i.e. the numbers of the aggregates verses the individual molecules) continues to increase as the water fraction increases. The increase of Φ_{FL} beyond 60% water content is consistent with an AIE process occurring in the nanoparticle dispersions (Table 1).

We next studied the photophysical properties in both PMMA and neat films. PMMA films were prepared from a casting solution of the respective TPE-DPA derivative in chloroform. The dilute solution was chosen to ensure that the molecules are spatially isolated within the PMMA host matrix. In the PMMA films, the Φ_{PL} values are considerably higher than when measured in solution (Table 1). This is attributed to suppression of non-radiative decay pathways, most likely internal rotation of the phenyl substituents in TPE, which causes the low Φ_{PL} in solution. This is supported by time-correlated single photon counting (TCSPC) measurements that show a clear increase in the timescale of the emission from the derivatives in the PMMA films compared with the THF solutions (Figure S5 and Table 2). In THF solutions and PMMA films, the TPE-DPA derivatives show double exponential decay behavior with the contribution of the longer-lived emission increasing from mono-, cis- to gem-DPA in THF and this term being a minor contributor in PMMA. We attribute the very short-lived component to a proportion of the molecules undergoing efficient non-radiative relaxation due to largely free rotational motion within the TPE core. Nevertheless, the curves in polyurethane films were well fit by single exponential functions. These results indicate that the active rotation of TPE core is restricted totally in polyurethane film. Interestingly, the Φ_{PL} in PMMA is higher than in the neat film of each derivative. While the precise reasons for this remain unclear, this observation could suggest that the neat films contain trap sites for singlet excitons, or regions where aggregation actually reduces the emission.

Table 1. PL quantum yield of TPE-DPA derivatives.

Compound	THF[a]	PMMA[b]	Neat[c]	NPs[d]
mono-DPA	0.01	0.84	0.64	0.57
cis-DPA	0.03	0.87	0.60	0.13
gem-DPA	0.01	0.88	0.48	0.30

[a] THF solution. [b] PMMA film (15 mM). [c] Neat film. [d] Nanoparticles.

Table 2. Photophysical properties of DPA and TPE-DPA derivatives.

Compound	ε[a]	τ_{PL} (ns)[b]	τ_{PL} (ns)[c]	τ_{PL} (ns)[d]	τ_t (μs)[e]	τ_t (μs)[f]	k_{SV} [g]
mono-DPA	28300	0.005/4.7	0.070/4.7	3.3	0.69	75	14.9
cis-DPA	30100	0.054/3.2	0.177/4.4	3.5	0.05/1.13	92	3.5
gem-DPA	17600	0.005/2.4	0.089/4.4	3.5	0.97	88	7.0

[a] Molar absorption coefficient ($M^{-1}cm^{-1}$) at 375 nm. [b] PL lifetime in THF solution. [c] PL lifetime in PMMA film. [d] PL lifetime in polyurethane (PU) film. [e] Triplet lifetime in THF solution. [f] Triplet lifetime in polyurethane thin film. [g] Stern-Volmer quenching constant ($\times 10^3$ M^{-1}) for the quenching of the phosphorescence of PtOEP in polyurethane thin film.

The Φ_{PL} of nanoparticle dispersions in water was also measured in light of the TTA-UC investigation (see the following section and experimental section for details). There was substantial variation in the Φ_{PL} of the TPE-DPA compounds compared to their neat samples and we attribute this to differences in sample preparation and therefore aggregation and crystallinity of the samples. Further investigation is required to gather evidence for and elucidate the exact cause of the differences. It should also be noted that the Φ_{PL} of TPE-DPA compounds in polyurethane could not be measured due to the overlap in the absorption spectra of the fluorophores and the matrix.

TTA-UC study

AIE materials are very attractive for TTA-UC applications, particularly in solid-state devices since solid-state TTA-UC requires high chromophore concentration to achieve high Φ_{PL}. AIE materials such as (2Z,2'Z)-2,2'-(1,4-phenylene)bis(3-phenylacrylonitrile) and 9,10-distyrylanthracene (DSA) have been used as emitters in TTA-UC systems.[24, 25] Given that DPA is an ideal emitter for TTA-UC[5, 26-28], we thus determined whether the TPE-DPA derivatives could be used as emitters for solid-state TTA-UC.

The triplet excited state properties of the compounds were investigated in both THF solution and a polyurethane matrix. The polyurethane matrix was chosen as it has been reported to be an effective host for solid-state upconversion studies.[5] Each derivative was able to effectively quench the phosphorescence of the well-known triplet sensitizer PtOEP (Figure 5a and Figure S9) in polyurethane films. For mono-DPA, the Stern-Volmer quenching constant (k_{SV}) is 14.9×10^3 M^{-1}, which is much higher than that of cis- and gem-DPA (3.5×10^3 M^{-1} and 7.0×10^3 M^{-1}, respectively) (Table 2). The higher Stern-Volmer quenching constant of mono-DPA indicates better mixing of PtOEP and mono-DPA in the polyurethane matrix.

Triplet lifetimes of the TPE-DPA derivatives were determined by flash photolysis of THF solutions and polyurethane films of the samples (Figure S6, Figure S7 and Table 2). In THF solution, mono- and gem-DPA show single exponential decays with lifetimes of 0.69 μs and 0.97 μs, respectively. cis-DPA has a double exponential decay with a major component of 1.13 μs. The TPE-DPA derivatives have much longer triplet lifetimes in polyurethane film (75 μs, 92 μs and 88 μs for mono-, cis- and gem-DPA, respectively) when compared with THF solution. This is consistent with the suppression of intramolecular rotation of TPE phenyl rings in the solid-state, which reduces non-radiative decay of the triplet population. These triplet lifetimes are much shorter than that of DPA (1 ms) both in solution and solid-state (Figure S8), which indicates that TPE chromophores decreases the triplet lifetime of TPE-DPA derivatives. We note here that the hydrophilic nature of polyurethane should result in aggregation of the hydrophobic fluorophores and dark field microscope images of the films confirmed the presence of particles in the micron size range (Figure S4). The measured triplet lifetimes are therefore affected by both intramolecular and intermolecular decay processes. Nevertheless, the triplet lifetimes of the TPE-DPA derivatives are comparable to those reported for other solid-state TTA upconversion systems employing related AIE-luminogens as emitters.[24, 25, 29]

To investigate solid-state TTA-UC in these materials, polyurethane samples containing the TPE-DPA compounds and PtOEP were first examined under 532 nm laser excitation. Unfortunately, the upconverted emission could not be observed in our instrumentation. As an alternative, THF solutions of TPE-DPA derivatives and PtOEP were co-precipitated in water in the presence of a surfactant, sodium dodecylsulfate (SDS), forming binary nanoparticle aqueous dispersions (see experimental section for sample preparation details). The average size of nanoparticles for mono-, cis- and gem-DPA are 243.8 nm, 353.9 nm and 311.5 nm, respectively (Figure S10).

As shown in Figure 5b, gem-DPA has the most intense upconverted emission, whereas the upconverted emission from mono-DPA is relatively weaker. This is despite having a high Φ_{PL} of 0.57 (Table 1), which is more than sufficient for efficient upconversion. The observation of upconversion in the binary TPE-DPA/PtOEP nanoparticles was confirmed by time-resolved PL measurements (Figure 6). Under 532 nm excitation, the blue upconversion emission at 452 nm shows the expected complex decay dynamics. The shorter-lived upconversion emission reflects the characteristic lifetime of the singlet state of the TPE-DPA derivatives. The longer-lived upconversion emission is a

consequence of the continued population of the emitter singlet state as a result of TTA occurring through continuing population and annihilation of the emitter triplets, which will be influenced by the lifetime of the triplet state of the sensitizer. Looking forward, the incorporation of these upconverting nanoparticles into water soluble matrices, such as polyvinyl alcohol (PVA), should result in solid state upconversion devices.

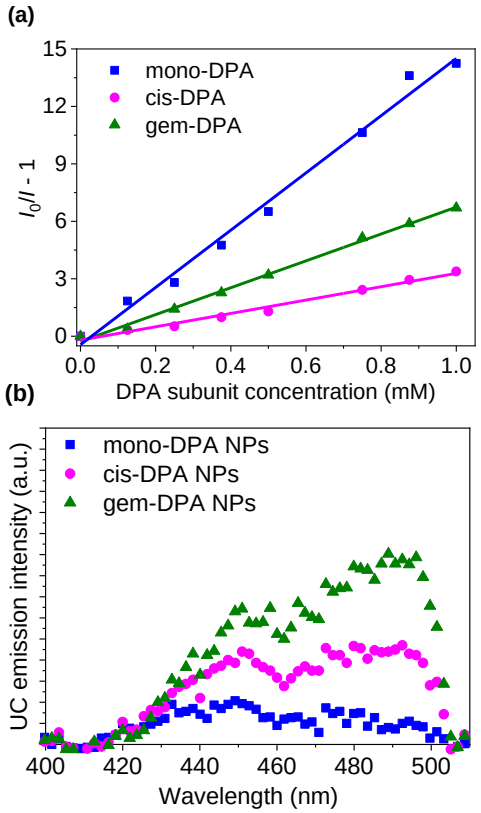

Figure 5. Stern-Volmer quenching of PtOEP (0.1 mM) in polyurethane film as a function of DPA subunit concentration (a); TTA upconversion emission of NPs aqueous dispersion excited by a 532 nm laser. Power density: 5000 mW/cm^2 (b).

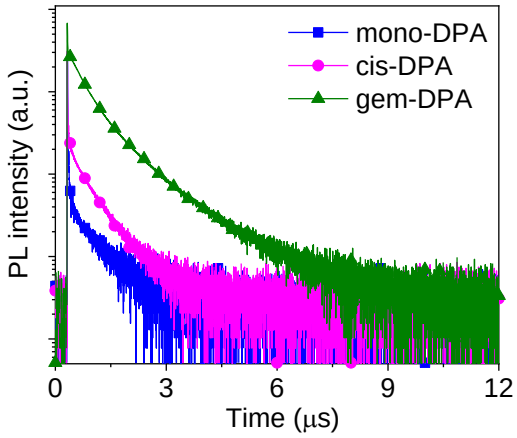

Figure 6. Upconverted emission decay of mono-, cis- and gem-DPA nanoparticles at 452 nm under 532 nm excitation.

An interesting outcome of the TTA-UC study is the observation that upconverted emission from mono-DPA is weakest, despite having a higher Φ_{PL} of 0.57 compared to the other TPE-DPA derivatives (Table 1). However, mono-DPA showed the shortest triplet excited state lifetime (Table 2) which would have a negative impact on the triplet-triplet annihilation process. As discussed earlier, the shortened triplet excited lifetime is mostly due to the presence of the TPE chromophore. Another interesting result was obtained when we measured the solution upconversion efficiency after the samples were irradiated in the presence of oxygen. On the basis of previous reports, TPE is susceptible to reaction with singlet oxygen to form a 1,2-endoperoxide adduct.[30] For each aerated solution, increased upconverted emission was observed after irradiation for 240 minutes (Figure 7). We hypothesized that, after irradiation, the TPE moiety was destroyed leaving the DPA moiety to participate in the TTA-UC process. As discussed earlier, all TPE-DPA derivatives were only weakly photoluminescent in solution because of the rotational non-radiative decay pathway of TPE.

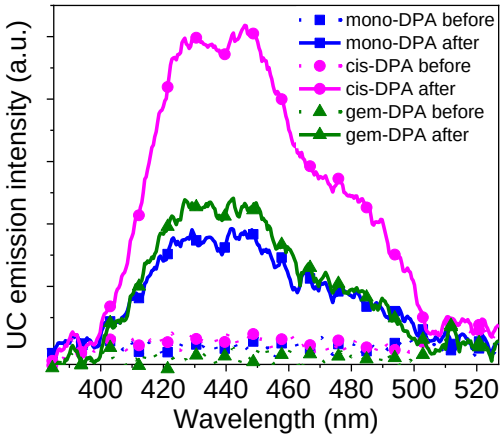

Figure 7. TTA upconversion emission of mono-, cis- and gem-DPA before and after 240 min irradiation in THF solution. TTA upconversion excitation power density: 5000 mW/cm^2 at 532 nm. [PtOEP]: 0.1 mM, [mono-DPA]: 2.5 mM, [cis-DPA]: 1.25 mM, [gem-DPA]: 1.25 mM.

Oxygen stability study

To further investigate the effect of oxygen on the photophysics of the TPE-DPA derivatives, we measured the stability of the TPE-DPA derivatives under constant irradiation by UV light. In dilute THF solutions, the TPE-DPA derivatives are almost non-emissive due to rotation of phenyl rings within the TPE moiety. Interestingly, emission from each TPE-DPA derivative increased significantly after irradiation (Figure 8 and Figure S11). This increase is despite possible oxidation of the anthracene core, which would reduce PL intensity.

To increase the rate of oxidation, PtOEP was added into the solutions. PtOEP is a widely used triplet photosensitizer due to its near-unity intersystem crossing efficiency[31, 32], and thus more singlet oxygen was generated in the mixed solution. The fluorescence emission intensity of mono-, cis- and gem-DPA increased at different rates in the different PtOEP solutions (Figure 8a for gem-DPA and see Figure S11 for mono- and cis-DPA). At lower PtOEP concentration (1 μM), the fluorescence of mono-, cis- and gem-DPA increased 22, 12 and 11 times, respectively, compared to the absence of the sensitizer. At higher PtOEP concentration (5 μM), the fluorescence of mono-, cis- and gem-DPA increased 25, 17 and 30 times, respectively. These results indicated that in gem-DPA, the TPE moiety is more easily oxidized with increased concentration of PtOEP.

The fluorescence emission intensity of mono-, cis- and gem-DPA increased throughout the course of the experiment (Figure 8 and Figure S11). At longer irradiation times, the emission intensity of cis- and gem-DPA reached a nearly constant value, suggesting that the TPE moiety had been fully oxidized. At the same time, the DPA moiety could also be oxidized to form an endoperoxide adduct which would decrease the PL emission intensity. The Φ_{PL} of each TPE-DPA derivative was measured after four hours irradiation, which are 0.09, 0.16 and 0.14 for mono-, cis- and gem-DPA, respectively (Table S2).

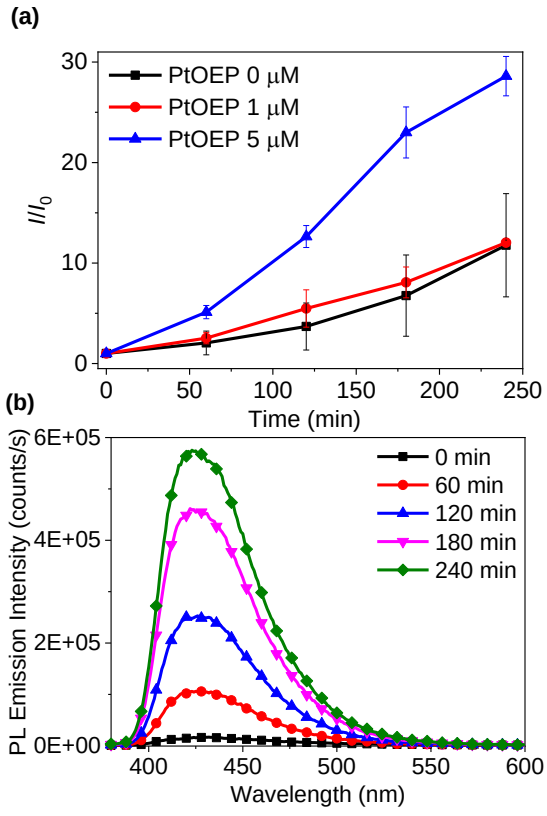

Figure 8. The variation of integrated fluorescence emission intensity of gem-DPA as a function of irradiation time (a); Time dependent enhancement of the PL intensity under irradiation of [gem-DPA]: 2.5 μM, [PtOEP]: 5 μM (b).

On the basis of these results, two possible oxidation routes are proposed for TPE-DPA derivatives (Scheme 2). Before irradiation, the mono-DPA is almost non-fluorescent due to phenyl ring rotation within the TPE moiety. Following irradiation, weak intersystem crossing in mono-DPA creates a triplet population that is able to sensitize formation of highly reactive singlet oxygen ($^1O_2$). The photosensitized $^1O_2$ can react with both TPE and DPA to form the endoperoxide (EP) adducts shown in Routes 1 and 2, respectively. These EP adducts were observed by mass spectrometry but were not isolated (Figure S12). Our results indicate that Route 1 is favoured since fluorescence intensity increases with irradiation time in each case.

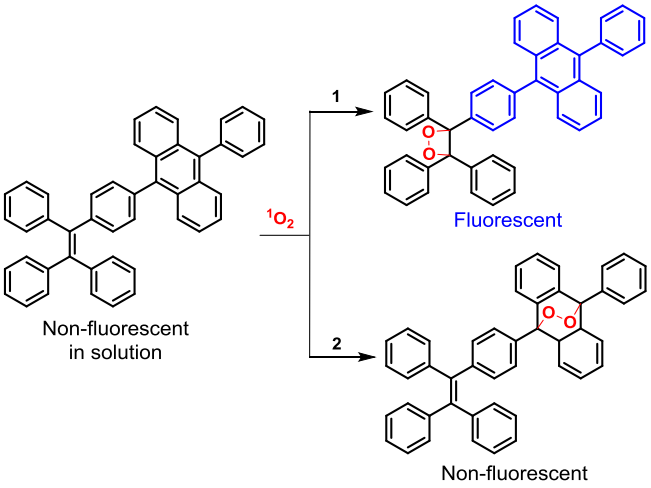

Scheme 2. Proposed oxidation products of mono-DPA.

Conclusions

A series of TPE-DPA derivatives that displayed AIE behaviour were designed and synthesized. In water:THF mixtures, the photoluminescence from each derivative was found to increase as the proportion of water increased, consistent with the expected behavior of AIE luminogens. When the derivatives were spatially isolated in PMMA films, a higher photoluminescence yield was observed than in solution or neat films. Interestingly, the solution samples exhibited enhanced TTA-UC emission under aeration and UV irradiation conditions. This phenomenon could be attributed to the oxidation of the TPE core to the 1,2-endoperoxide adduct, which effectively 'switches on' photoluminescence from the samples. Upconverted emission was observed in aqueous nanoparticle dispersions of the TPE-DPA derivatives and PtOEP, thus demonstrating the potential of this molecular design for solid-state upconversion.

Experimental Section

Synthesis of TPE-DPA derivatives

Synthesis of mono-DPA: A mixture of 4,4,5,5-tetramethyl-2-(4-(1,2,2-triphenylvinyl)phenyl)-1,3,2-dioxaborolane (200 mg, 0.436 mmol), 9-bromo-10-phenylanthracnene (174 mg, 0.524 mmol), Pd(PPh3)4 (25.2 mg, 0.0218 mmol) was degassed for 30 mins. Once the mixture has been fully deaerated, degassed toluene (2% w/v Aliquat 336, 10 mL) and degassed 2 M K_2CO_3 was added into the reaction. The reaction mixture was left stirring overnight at 80˚C. Upon reaction condition, the mixture was washed with dichloromethane, H_2O and brine solution. The organic layer was then collected and dried using $MgSO_4$. The mixture was then filtered and the solvent was removed before the desired product was isolated by silica gel column chromatography using 3:7 v/v DCM : PET as eluent. The desired product was obtained as bright yellow crystalline needles with 69% yield (70 mg). Melting Point: 291-297˚C. ^{1}H NMR (400 MHz, $CDCl_3$) δ (ppm): 7.67 (ddt, 4H), 7.62 - 7.51 (m, 3H), 7.49 - 7.43 (m, 2H), 7.38 - 7.29 (m, 4H), 7.29 - 7.11 (m, 19H). ^{13}C NMR (100MHz, CDCl3) δ (ppm): 143.88, 143.47, 143.35, 143.09, 141.54, 140.96, 139.05, 131.52, 131.36, 131.29, 131.23, 130.56, 129.82, 129.73, 128.36, 127.79, 127.70, 127.57, 127.41, 126.96, 126.58, 126.54, 124.93, 124.85. FTIR (cm^{-1}): 3060, 3019, 1600, 1493, 1443, 1392. MALDI-TOF (m/z): Calculated for $C_{46}H_{32}$: 584.2504. Found: 584.1329.

Synthesis of cis-DPA: A mixture of (Z)-1,2-diphenyl-1,2-bis(4,4,5,5-tetramethyl-1,3,2-dioxaborolan-2yl)ethene (48 mg, 0.244 mmol), 9-(4-Bromophenyl)-10-phenylanthracene (100 mg, 0.244 mmol), $Pd(PPh_3)_4$ (4 mg, 0.003 mmol) was added to degassed toluene (equipped with 2% w/v Aliquat 336, 5 mL) and 2 M K_2CO_3 (5 mL). The reaction mixture was refluxed under nitrogen atmosphere at 90˚C overnight. Upon cooling to room temperature, the reaction mixture was quenched with H_2O and the organic layer was extracted using dichloromethane and dried with $MgSO_4$. After filtration, the solvent was removed and the remaining residue was recrystallised using dichloromethane and isopropyl alcohol to give the desired product as pale yellow solid (35 mg, 38%). Melting Point: 366-368˚C. ^{1}H NMR (600MHz, $CDCl_3$) δ (ppm): 7.69 (dt, 4H), 7.64 (dt, 4H), 7.61 - 7.55 (m, 4H), 7.55 - 7.51 (m, 2H), 7.50 - 7.41 (m, 8H), 7.40 - 7.30 (m, 9H), 7.29 - 7.26 (m, 3H), 7.24 - 7.17 (m, 6H), 7.04 (ddd, 4H). ^{13}C NMR ($CDCl_3$, 100MHz) δ (ppm): 143.49, 143.24, 141.45, 139.09, 137.33, 136.86, 131.51, 131.47, 131.31, 130.71, 129.77, 128.35, 127.88, 127.41, 126.79, 126.72, 125.17, 124.87, 109.99. FTIR (cm^{-1}): 3060, 3028, 1600, 1506, 1500, 1443, 1389, 1370. MALDI-TOF (m/z): Calculated for $C_{66}H_{44}$: 836.3443. Found: 836.3624.

Synthesis of gem-DPA: A mixture of 2,2'-((2,2-diphenylethene-1,1-diyl)bis(4,1-phenylene))bis(4,4,5,5-tetramethyl-1,3,2-dioxaborolane) (700 mg, 1.19 mmol), 9-bromo-10-phenylanthracene (1.19 g, 3.59 mmol) and $Pd(PPh_3)_4$ (5 mol%, 70 mg) was kept under inert atmosphere for 30 mins before degassed K_2CO_3 (2 M solution, 20 mL) and degassed toluene (2% w/v Aliquat 336, 40 mL) was added into mixture. The mixture was refluxed overnight under nitrogen atmosphere. Upon cooling, water was added to the mixture and the organic layer was further extracted with DCM and washed with brine. The organic layer was then dried using $MgSO_4$. The crude product was then crystallised using chloroform to yield pale yellow precipitates (0.622 g, 62 %). Product decomposed at 350˚C as it turned brown. ^{1}H NMR (400MHz, $CDCl_3$) δ (ppm): 7.73 (dt, 4H), 7.69 (dt, 4H), 7.60 (tt, 4H), 7.57 - 7.53 (m, 2H), 7.49 - 7.45 (m, 8H), 7.38 (ddd, 4H), 7.36 - 7.29 (m, 8H), 7.29 - 7.26 (m, 7H), 7.24 - 7.19 (m, 2H). ^{13}C NMR ($CDCl_3$, 100MHz) δ (ppm): 143.71, 142.72, 142.23, 141.01, 139.07, 137.24, 137.02, 131.60, 131.37, 131.31, 130.80, 129.86, 129.79, 128.39, 127.68, 127.44, 127.00, 126.96, 126.71, 124.98, 124.92. FTIR (cm^{-1}): 3048, 1440, 1393, 1374. MALDI-TOF (m/z): Calculated for $C_{66}H_{44}$: 836.3443. Found: 836.3922.

The synthesis details of the intermediate products and general procedures are described in the Supporting Information. CCDC 1896079-1896081 contains the supplementary crystallographic data for this paper. These data can be obtained free of charge from The Cambridge Crystallographic Data Centre via www.ccdc.cam.ac.uk/data_request/cif.

Sample preparations

Samples for absolute Φ_{PL} measurements in PMMA were prepared by drop casting 0.1 mL of a casting solution of the TPE-DPA derivatives and PMMA on top of the 1.25 cm × 1.25 cm × 0.1 cm glass slides. The glass slides were washed thoroughly before used. The casting solutions of the TPE-DPA derivatives and PMMA were prepared by diluting the mixture of the prototypical solutions in $CHCl_3$ of each compound and the PMMA solution (0.05 g/ml in $CHCl_3$) with $CHCl_3$ to reduce the concentration of PMMA to 1% w/w. The concentration of the TPE-DPA derivatives in the casting solutions were calculated based on the volume of the solid-state PMMA. After drop casting, the samples were dried under room temperature for 5 h and then baked at 100 ˚C for 10 min to evaporate the solvent. Samples for absolute Φ_{PL} measurements in neat conditions were prepared by drop casting dilute TPE-DPA derivative THF solution on top of the 1.25 cm × 1.25 cm × 0.1 cm glass slides.

Samples for Stern-Volmer quenching measurement were prepared in polyurethane following the procedure in the literature.[5] The commercially available polyurethane precursor, which is composed of two parts - polyol and diisocyanate - was purchased under the trade name Clear Flex 50®, from Smooth-on, Inc. Polyurethane films were prepared as follows: polyester polyol (1600 µL, component B in Clear Flex 50®) and methylene bis (4- cyclohexyl isocyanate (800 µL, component A in Clear Flex 50®) were mixed with PtOEP solution dissolved in THF (800 µL, 0.3 mM). After thorough mixing, 150 µL aliquots of the mixture were distributed to ten separated glass vials. Various volumes of the TPE-DPA derivative in THF (varying from 0 to 100 µL) were added to each vial, the mixture was cast onto a square microscopy cover glass (size: 22 × 22 mm) and then another cover glass was carefully mounted on the mixture in order to make a flat and even polymer film. After curing for 12 hours at room temperature, the samples were subsequently placed in a vacuum oven at 60 ˚C for 12 hours to completely remove residual THF from the films. The samples containing PtOEP (0.1 mM) and the DPA subunit (0 to 1.25 mM) were used for Stern-Volmer quenching studies.

Preparation of the TPE-DPA NPs: TPE-DPA derivatives in THF (1.5 mM, 2 mL) was added dropwise into 10 mL of 10 mM sodium dodecyl sulfate (SDS) aqueous solution. The mixture was stirred vigorously at room temperature overnight to completely volatilize the THF.

Preparation of the UC NPs: A mixture of TPE-DPA (1.5 mM, 2 mL) and PtOEP (1 mM, 15 μL) in THF was added dropwise into 10 mL of 10 mM SDS aqueous solution. The mixture was stirred vigorously at room temperature overnight to completely volatilize the THF.

The samples for oxidation in dilute solutions were prepared in THF in 7 mL vials. For each sample, three identical samples were prepared. The samples were irradiated under a UV LED with the maximum emission peak at 364 nm with the power density of 19.8 mW/cm^2 in an aerated condition. The emission intensity was measured on the Varian Cary Eclipse fluorimeter every 60 minutes.

Samples containing PtOEP (0.1 mM) and the DPA subunit (1.25 mM) were used for flash photolysis measurement in polyurethane films. Samples for flash photolysis measurement in THF solution and samples of NPs aqueous solution for upconversion measurement were degassed by using freeze-pump-thaw method for three cycles.

Optical measurements

Steady-state absorption and PL spectra were recorded on a Cary 50 UV-vis spectrophotometer and Varian Cary Eclipse fluorimeter, respectively. For the PL spectra, the excitation wavelength was 375 nm for DPA, mono-, cis- and gem-DPA, 320 nm for TPE. Relative Φ_{PL} was determined by using DPA as a standard in dilute THF solution. Absolute Φ_{PL} values in PMMA and neat film were measured using a calibrated integrating sphere (F-3018) accessory on a FluoroLog-3 fluorimeter using a broadband xenon arc lamp light sauce. Stern-Volmer quenching dynamics were investigated as a function of sensitizer concentration and emitter in polyurethane film, which were measured by exciting with a 532 nm CW laser and spectrally detecting the emission using an Ocean Optics (HR2000) optical fibre-based spectrometer. Fluorescence decay measurements of the emitters were acquired on a time correlated single photon counting (TCSPC) setup using the frequency doubled output of a mode-locked and cavity dumped Ti:Sapphire laser (Coherent Mira 900F/APE PulseSwitch) with excitation at 405 nm. Triplet decay measurements of the emitters were determined on a nanosecond flash photolysis setup by exciting at 532 nm (Ekspla NT340, operating at 10 Hz) and monitoring at 452 nm. The probe light source was a MCWHLP1 Thorlabs broadband LED with DC2200 controller to generate 10ms pulses at 10 Hz, synchronized with pump laser. The intensity of the transmitted light as a function of time was recorded on a R928 Hamamatsu PMT detector and Tektronix (TDS520) digital storage oscilloscope over 500 averages. The scattering images of crystals in polyurethane films were collected with a Nikon Lv100 Eclipse inverted micro-scope, equipped with a dark-field condenser and LU plus ELWD 20×/0.55 Nikon lens in the reflection configuration. The light source of the microscope was a 100 W quartz halogen lamp. A CCD Camera (ThorLabs) was attached to the microscope to capture the dark-field images.

Acknowledgements

This work was made possible by support from the Australian Renewable Energy Agency which funds the project grants within the Australian Centre for Advanced Photovoltaics (ACAP). WWHW was supported by an ARC Future Fellowship (FT130100500). TAS and WWHW are supported by the ARC Centre of Excellence in Exciton Science (CE170100026). The authors also thank the Australian Synchrotron for beamtime via the Collaborative Access Program (proposal number 13618b).

Keywords: aggregation-induced emission • anthracene • photoluminescence • photon upconversion • tetraphenylethene

[1] J. Yang, J. Huang, Q. Li, Z. Li, *J. Mater. Chem. C*. **2016**, *4*, 2663-2684.
[2] D. Ding, K. Li, B. Liu, B. Z. Tang, *Acc. Chem. Res.* **2013**, *46*, 2441-2453.
[3] J. Mei, N. L. C. Leung, R. T. K. Kwok, J. W. Y. Lam, B. Z. Tang, *Chem. Rev.* **2015**, *115*, 11718-11940.
[4] D. Dzebo, K. Börjesson, V. Gray, K. Moth-Poulsen, B. Albinsson, *J. Phys. Chem. C*. **2016**, *120*, 23397-23406.
[5] J. Kim, F. Deng, F. N. Castellano, J. Kim, *Chem. Mater.* **2012**, *24*, 2250-2252.
[6] C. E. McCusker, F. N. Castellano, *Top Curr. Chem.* **2016**, *374*, 175-199.
[7] A. Monguzzi, M. Frigoli, C. Larpent, R. Tubino, F. Meinardi, *Adv. Funct. Mater.* **2012**, *22*, 139-143.
[8] V. Gray, D. Dzebo, A. Lundin, J. Alborzpour, M. Abrahamsson, B. Albinsson, K. Moth-Poulsen, *J. Mater. Chem. C*. **2015**, *3*, 11111-11121.
[9] S. Kabilan, W. M. Rowan, R. P. Joshua, Y. C. Yuen, D. Miroslav, R. M. Dane, D. T. Neil, S. Natalie, W. S. Timothy, *J. Mater. Chem. C*. **2015**, *3*, 616-622.
[10] Y. J. Bae, G. Kang, C. D. Malliakas, J. N. Nelson, J. Zhou, R. M. Young, Y. Wu, R. P. Van Duyne, G. C. Schatz, M. R. Wasielewski, *J. Am. Chem.Soc.* **2018**, *140*, 15140-15144.
[11] P. C. Boutin, K. P. Ghiggino, T. L. Kelly, R. P. Steer, *J. Phys. Chem. Lett.* **2013**, *4*, 4113-4118.
[12] A. J. Tilley, M. J. Kim, M. Chen, K. P. Ghiggino, *Polymer*. **2013**, *54*, 2865-2872.
[13] A. J. Tilley, B. E. Robotham, R. P. Steer, K. P. Ghiggino, *Chem. Phys. Lett.* **2015**, *618*, 198-202.
[14] Z. Zhao, P. Lu, J. W. Y. Lam, Z. Wang, C. Y. K. Chan, H. H. Y. Sung, I . D. Williams, Y. Ma, B. Z. Tang, *Chem. Sci.* **2011**, *2*, 672-675.
[15] S. Kim, Y. Park, I. Kang, J. Park, *J. Mater. Chem.* **2007**, *17*, 4670-4678.
[16] K. C. C. Y, J. W. Y. Lam, Z. Zhao, C. Deng, S. Chen, P. P. Lu, H. H. Y. Sung, H. S. Kwok, Y. Ma, I. D. Williams, B. Z. Tang, *ChemPlusChem.* **2012**, *77*, 949-958.
[17] J. Wang, J. Mei, R. Hu, J. Z. Sun, A. Qin, B. Z. Tang, *J. Am. Chem. Soc.* **2012**, *134*, 9956-9966.
[18] Y. Dong, J. W. Y. Lam, A. Qin, J. Liu, Z. Li, B. Z. Tang, J. Sun, H. S. Kwok, *Appl. Phys. Lett.* **2007**, *91*.
[19] Z. Zhao, J. W. Y. Lam, B. Z. Tang, *J. Mater. Chem.* **2012**, *22*, 23726-23740.
[20] S. Biswas, D. Jana, G. S. Kumar, S. Maji, P. Kundu, U. K. Ghorai, R. P. Giri, B. Das, N. Chattopadhyay, B. K. Ghorai, S. Acharya, *ACS Appl. Mater. Interfaces*. **2018**, *10*, 17409-17418.
[21] B. Zhang, J. L. Banal, D. J. Jones, B. Z. Tang, K. P. Ghiggino, W. W. H. Wong, *Mater. Chem. Front.* . **2018**, *2*, 615-619.
[22] B. Zhang, C. Gao, S. N. Neto, W. W. H. Wong *Principles and applications of aggregation-induced emission, (Eds: Y. Tang, B. Z. Tang)*, *Springer*. **2019**, pp. 479-504.
[23] T. Serevicius, R. Komskis, P. Adomenas, O. Adomeniene, V. Jankauskas, A. Gruodis, K. Kazlauskas, S. Jursenas, *Phys. Chem. Chem. Phys.* **2014**, *16*, 7089-7101.
[24] P. Duan, N. Yanai, Y. Kurashige, N. Kimizuka, *Angew. Chem. Int. Ed.* **2015**, *54*, 7544-7549.
[25] L. Li, Y. Zeng, T. Yu, J. Chen, G. Yang, Y. Li, *ChemSusChem*. **2017**, *10*, 4610-4615.
[26] S. Hisamitsu, N. Yanai, N. Kimizuka, *Angew. Chem. Int. Ed.* **2015**, *54*, 11550-11554.
[27] N. Kimizuka, N. Yanai, M. A. Morikawa, *Langmuir*. **2016**, *32*, 12304-12322.
[28] N. Yanai, N. Kimizuka, *Chem. Commun.* **2016**, *52*, 5354-5370.
[29] Z. Qu, P. Duan, J. Zhou, Y. Wang, M. Liu, *Nanoscale*. **2018**, *10*, 985-991.
[30] K. Ohkubo, T. Nanjo, S. Fukuzumi, *Org. Lett.* **2005**, *7*, 4265-4268.
[31] J. Zhao, S. Ji, H. Guo, *RSC Adv.* **2011**, *1*, 937-950.
[32] J. Zhou, Q. Liu, W. Feng, Y. Sun, F. Li, *Chem. Rev.* **2015**, *115*, 395-465.

Entry for the Table of Contents

FULL PAPER

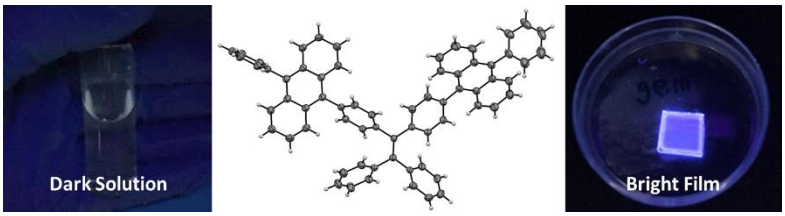

Tetraphenylethene 9,10-diphenylanthracenes (TPE-DPAs) were synthesized and characterized. The TPE-DPAs displayed aggregation induced emission behaviour and were shown to work as emitters in nanoparticle triplet-triplet annihilation upconversion systems with platinum porphyrin as triplet sensitizer.

Can Gao, Jia Yi Seow, Bolong Zhang, Christopher Hall, Andrew J. Tilley, Jonathan M. White, Trevor A. Smith, and Wallace W. H. Wong**

Page No. – Page No.

Tetraphenylethene 9,10-Diphenylanthracene Derivatives – Synthesis and Photophysical Properties